On the variations of acoustic absorption peak with particle velocity in Micro-Perforated Panels at high level of excitation

Rostand Tayong, Thomas Dupont, Philippe Leclaire

On the variations of acoustic absorption peak with particle velocity in Micro-Perforated Panels at high level of excitation

R. Tayong, T. Dupont and P. Leclaire
Laboratoire de Recherche en Mécanique et Acoustique (DRIVE-LRMA),
ISAT - Université de Bourgogne, 49 Rue Mademoiselle Bourgeois 58027 Nevers cedex, France
e-mail: **rostand.tayong@u-bourgogne.fr**

Abstract

The acoustic behavior of micro-perforated panels (MPP) is studied theoretically and experimentally at high level of pressure excitation. A model based on Forchheimer's regime of flow velocity in the perforations is proposed. This model is valid at relatively high Reynolds numbers and low Mach numbers. The experimental method consists in measuring the acoustical pressure at three different positions in an impedance tube, the two measurement positions usually considered in an impedance tube and one measurement in the vicinity of the rear surface of the MPP. The impedance tube is equipped with a pressure driver instead of the usual loudspeaker and capable of delivering a high sound pressure level up to 160 dB. MPP specimens made out of steel, dural and polypropylene were tested. Measurements using random noise or sinusoidal excitation in a frequency range between 200 and 1600 Hz were carried out on MPPs backed by air cavities. It was observed that the maximum of absorption can be a positive or a negative function of the flow velocity in the perforations. This suggests the existence of a maximum of absorption as a function of flow velocity. This behavior was predicted by the model and confirmed experimentally

1 Introduction

In various noise control applications, perforated panels are used to attenuate sound. These materials present very interesting sound absorption characteristics when the perforations sizes are reduced to millimeter or submillimeter size[1] (the term micro-perforated panel is rather used for submillimetric radius). Moreover, they are proved to be very useful in dealing with low-frequency noise. A large number of models[1, 2, 3] have been proposed to model the acoustical behavior of perforated and micro-perforated panels under low sound levels (known as the linear regime). In the case of high sound pressure excitation, it is thought that the jet formation (vorticity) at the opening modifies significantly the absorption mechanisms[4, 5]. Studies on perforates at medium and high sound pressure levels lead to understand the effect of high sound pressure on the performance of micro-perforated panels[6, 7]. This work is aimed at describing the acoustic absorption coefficient variations for microperforated panels (in the absence of mean flow) at high level of excitation. It uses a relatively simple linear model (Maa's model[1]) to end up describing the high sound level variations of the absorption coefficient. A dimensionless parameter involved in the MPP behavior is introduced. In this paper, it is noted that depending on the described dimensionless parameters that is found, the resulting absorption coefficient will either solely decrease with the increase of Mach number or in a first phase increase to a maximum level before decreasing in a second phase with the increase of Mach number. The validity of the presented theory is discussed by comparing prediction results obtained for normal incidence sound absorption coefficients.

2 Impedance and absorption coefficient model

2.1 Linear regime

The main mechanism of absorption in the linear regime is the conversion of the acoustical energy into heat. In this regime (low sound pressure and velocity amplitudes), if the dimensions of the MPP (diameter of holes, holes separation, thickness) are small with respect to the impinging acoustic wavelength, and if the aperture dimension (diameter of holes) is of the order of the viscous and thermal boundary layers thicknesses, the major part of the acoustical energy is dissipated through viscous and thermal effects. Based on the theory and equations of acoustical propagation in short and narrow circular tubes, Maa[1] derived an equation of aerial motion given for one perforation by

$$j\omega\rho_0 u - \frac{\eta}{r}\frac{\partial}{\partial r}\left[r\frac{\partial}{\partial r}u\right] = \frac{\Delta p}{h}, \tag{1}$$

where $\triangle p$ is the pressure drop across the tube, h the length of the tube (which corresponds to the thickness of the MPP), η the dynamic viscosity, ρ_0 the density of air, ω the angular frequency, r the radial coordinate and u the particle velocity in the perforation. By solving the equation with respect to the velocity, the specific acoustic impedance of the short tube defined as the ratio of $\triangle p$ to the average velocity $< u >$ over a cross-sectional area of the tube is given by:

$$Z_{perf} = \frac{\Delta p}{< u >} = j\omega\rho_0 h\left[1 - \frac{2}{x\sqrt{-j}}\frac{J_1(x\sqrt{-j})}{J_0(x\sqrt{-j}}\right]^{-1}, \tag{2}$$

where $x = d.\sqrt{\frac{\omega\rho_0}{4\eta}}$ is a constant defined as the ratio of orifice diameter d to the viscous boundary layer thickness of the air in the orifice, J_0 and J_1 the Bessel functions of the first kind of orders 0 and 1, respectively. An approximation of the above equation on the Bessel functions and valid for narrow tubes was given by Maa[1] as :

$$Z_{perf} = \frac{32\eta h}{d^2}\sqrt{1 + \frac{x^2}{32}} + j\omega\rho_0 h\left[1 + \frac{1}{\sqrt{3^2 + x^2/2}}\right]. \tag{3}$$

Due to the end radiating effects at the aperture, an end correction factor should be taken into account twice (once for each end). This correction is important when the perforation diameters are greater or of the order of the plate thickness[4]. The radiation impedance for an opened cylindrical tube is that of a piston in a baffle and is given by Morse[8] (for the case $k_0 d << 1$) and written as :

$$Z_{ray} = \frac{(k_0 d)^2}{2} + j\frac{8k_0 d}{3\pi}, \tag{4}$$

where k_0 is the wave number. The radiation impedance should be doubled accounting for each aperture side. The effect of the vibration of the air particles on the baffle in the vicinity of the aperture increases the thermo-viscous frictions. To take this effect into account, Rayleigh[9] proposed an additional factor on the resistive part of the tube impedance. This resistance is given by :

$$R_S = \frac{1}{2}\sqrt{2\omega\rho_0\eta}. \tag{5}$$

Under a certain number of assumptions, a process of homogenization can be applied, providing an expression of the impedance for multiple perforations. The minimal distance between perforations must be greater than their diameters and smaller than the wavelength and so it is possible to consider that there is no interactions between the apertures and the absorption mechanism is dominant. The MPP must be thinner than the wavelength to insure the continuity of the velocities on both sides of the plate. Within these assumptions, the visco-thermal interactions between the fluid and the solid are taken into account through a viscosity correction function[1]

The total impedance of the MPP is then given by the impedance of one perforation divided by the open area ratio ϕ :

$$Z_{MPP} = \frac{Z_{perf} + 2Z_{ray} + 4R_S}{\phi}, \tag{6}$$

The factor 4 in the previous expression accounts for the fact that the resistance R_S given by Rayleigh is too small in practice. Ingard[3] so as Allard[2] also observed this behavior in their models.

2.2 Nonlinear regime

From the semi-empirical approach of Ingard[3], we investigated a model based on dimensional analysis[10] in order to study the influence of the MPP geometrical parameters. This model is found to be consistent with including the Forchheimer nonlinear flow regime in the linear model. This approach was used by Auregan and Pachebat[11] for the study of nonlinear acoustical behavior of rigid frame porous materials. Following Ingard and Ising[4] work on the nonlinear behavior of perforates at high sound amplitudes, the real part of the characteristic impedance is given by

$$\mathrm{Re}\left\{z_{MPP}\right\}_{NL} = aM + b, \tag{7}$$

where z_{MPP} is the normalized impedance, a and b are dimensionless parameters that depend on the MPP geometrical features and on the fluid constants. First from a dimensional analysis and then a use of Forchheimer law, it is found that

$$a = K\frac{dc_0}{\nu\phi}, \tag{8}$$

where ν is the kinematic viscosity. It is found that the coefficient b is related to dimensionless coefficient δ of Auregan and Pachebat[11] through the relation :

$$b = (1+\delta)\mathrm{Re}\{z_{MPP}\}_{linear} \tag{9}$$

where δ is characteristic of 3 regimes : the linear regime ($\delta = 0$), the weakly nonlinear regime ($\delta \neq 0$) and a transition regime between them. The weakly nonlinear regime is asymptotically linear as M increases and therefore, b corresponds to the intercept of the straight line with the vertical axis (b has no real physical interpretation as for M=0, the asymptotic behavior does not hold). In this paper, both K and δ (or b) were determined from a linear fitting.

The normalized surface impedance of the total system (MPP coupled to an air cavity) is given by the superposition of the two impedances[1, 4]:

$$z_s = z_{MPP} + z_c, \tag{10}$$

where the normalized form of the impedance z_c of the air cavity is given by

$$z_c = -j\cot\left(k_0 D_c\right), \tag{11}$$

where D_c is the air gap thickness. The reflection coefficient is given by the usual formula

$$R = \frac{z_s - 1}{z_s + 1}. \tag{12}$$

and the acoustic absorption coefficient can be calculated from

$$\alpha\left(\omega\right) = 1 - \left|R\left(\omega\right)\right|^2. \tag{13}$$

2.3 Absorption peak variations

From the study of the variations of the absorption coefficient function, it is found that the peak of absorption (maximum of absorption with respect to frequency) increases with the Mach number, reaches a maximum as the Mach number approaches its critical value and then decreases for M increasing beyond the critical value M_c. The maximum of absorption is obtained for $Im\{z_s\} = 0$:

$$\alpha_M = \frac{4(aM+b)}{(1+aM+b)^2}. \tag{14}$$

Evidently, this behavior can be observed if the sample resistance is less than the medium resistance and practically very often if the critical value is above the linear/nonlinear regime limit. Indeed, the experimental results will show that in some cases, a value for M_c will not be identified if it is located in the linear range. In this case the MPP absorption peak will only decrease with the increasing sound pressure level. It is also worth noticing that $\alpha_M(M_c) = 1$ for any MPP with M_c located in the nonlinear domain.

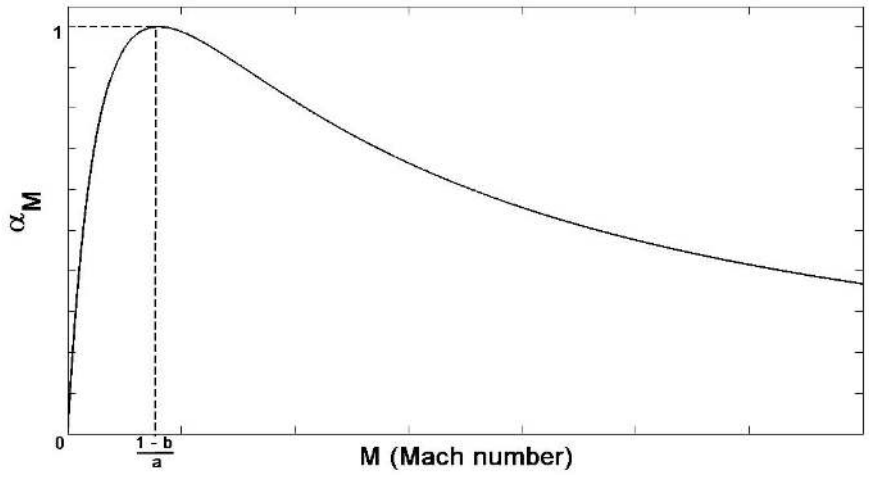

Figure 1: Absorption coefficient at the resonance frequency (α_M in expression (14)) versus the acoustical Mach Number in front of the MPP.

3 Experimental setup

3.1 Micro-perforated samples

The measurements are performed on strong copolymer-made MPP, steel-made and dural-made MPP (see Table 1 for the characteristics). All the samples have an external diameter of 100 mm and all the holes are well separated from each other (no interactions between the apertures) and are evenly distributed over the panel area. The mounting conditions of the MPP inside the tube are closer to the clamped conditions than to the simply supported conditions.

3.2 Experimental procedure

A schematic of the impedance tube used is shown in Fig. 2. It is a rigid circular plane-wave tube with a diameter of 100 mm. Plane wave propagation is assumed below the cut-off frequency of the impedance tube (about 1.7 KHz). At the left hand side, a compression driver JBL model 2450J is mounted as the source of excitation. A transition piece provides a continuity transition between the circular section of the compression

Table 1: Micro-perforated panel characteristics.

	h (mm)	d (mm)	ϕ (%)	Density (Kg/m^3)	Young Modulus (Pa)	Material
MPP1	2.2	1.0	2.2	900	0.49×10^{10}	Strong copolymer
MPP2	2.2	1.0	0.8	900	0.49×10^{10}	Strong copolymer
MPP3	2.0	0.7	1.94	7800	21×10^{10}	Steel
MPP4	2.0	1.0	1.6	2700	0.69×10^{10}	Dural

driver and the circular cross section of the plane-wave tube. At the right hand side of the tube, a soundproof plunger is used as the rigid backing wall. By moving the plunger along the longitudinal axis of the tube, one is able to create an air cavity behind the MPP sample. The MPP sample is mounted between the speaker and the plunger. Three $1/4''$ microphones are used to perform the signal detection. Two microphones are used to calculate the surface impedance of the sample by the standard impedance tube measurement technique[13]. The third microphone (reference micro in Fig. 2) acts as a reference microphone to get the level of pressure at the sample surface. The measurement are carried out at high sound pressure levels. However, assuming

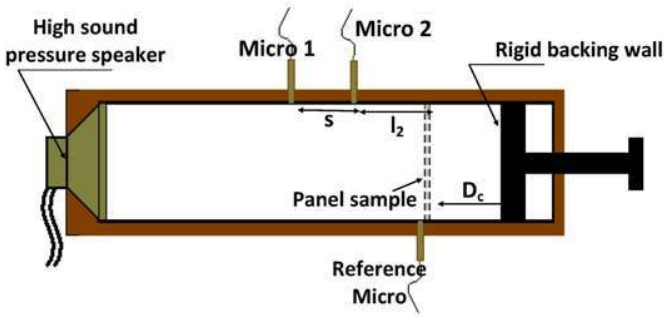

Figure 2: Schematic of the impedance tube used for the measurements.

the plane wave hypothesis, one can measure the pressures and velocities on any section of the tube using the two microphone method. See for instance Dalmont[14] for more details. The acoustic velocity on the panel surface is given by:

$$u = j\frac{p_1}{Z_0}\frac{H\cos(k_0 l_1) - \cos(k_0 l_2)}{\sin(k_0 s)}, \tag{15}$$

where l_1=s+l_2 as in Fig. 2. H is the ratio of pressures measured on two points of the tube. Z_c is the characteristic impedance of air, k_0 is the wave number, p_1 is the pressure on microphone 1, and l_1 (resp. l_2) is the distance from microphone 1 (resp. 2) to the panel sample. The values of the velocity shown in the experimental results are the viscous peak corresponding particle velocity.

4 Results and discussion

4.1 Theory and experiment for α_M as a function of M

The dimensionless parameters K and δ used to fully determine expression (7) are given in Table 2. Fig. 3 shows the comparison between experimental results and the present model simulations for the resistance as a function of the Mach number for all the MPP samples. The air cavity depth is 50 mm. The experiments and the present model are in good agreement for the high excitation levels. This result points out the fact that for high sound pressure levels, the dependency of the resistance and the Mach number is linear. The slope is different from one MPP to another, revealing therefore the fact that this slope, in the same measurement

Table 2: Dimensionless parameters of the microperforated panels.

	M_c	K	δ
MPP1	0.18×10^{-3}	1.43×10^{-3}	2.024
MPP2	0.22×10^{-3}	1.43×10^{-3}	3.868
MPP3	Not observable	1.56×10^{-3}	0.956
MPP4	9.41×10^{-5}	2.2×10^{-3}	0.8

conditions, depends on the MPP geometrical parameters. This result also shows that the value of constant K seems to be related to the type of material (1.43×10^{-3} for the copolymer samples, 1.56×10^{-3} for the steel sample, 2.2×10^{-3} for the dural sample), and as already mentioned, to the shape of the aperture edge. Fig. 4

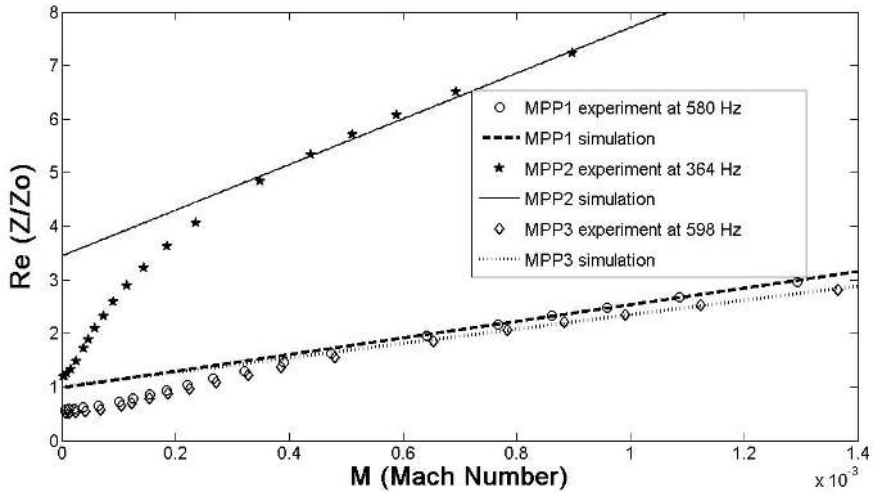

Figure 3: Surface impedance resistive part as a function of the Mach number in front of the MPP sample. Air cavity depth of 50 mm.

shows the comparison between experimental results and the present model simulations for the maximum absorption coefficient versus the Mach number for MPP1, MPP2 and MPP3 samples. The air cavity depth is 50 mm. The experiments and the simulation are in fairly good agreement. This confirms the fact that depending on the value of the limit Mach number with the increase of sound levels, the absorption peak will in a first phase rise up to a maximum value before, in a second phase, decreasing. It should be pointed out that for the three cases presented, as already mentioned in the theoretical part, the maximum of α_M cannot be predicted theoretically because the limit Mach number M_c is below the linear/nonlinear limit regime. The limit Mach number is observable experimentally on MPP1 and MPP3 (the values of the maximum are given in Table 2) in a region where the proposed model is not valid and therefore the maximum cannot be predicted theoretically. For MPP2, the maximum could neither be observed experimentally nor predicted. In fact, if this limit Mach number is low, the absorption peak will solely decrease with the increase of sound pressure levels. Fig. 5 shows the comparison between experimental results and present model for another MPP (MPP4). This example illustrates the case where the maximum of α_M is observable theoretically, because the critical Mach number is predicted in the domain of validity of the model. The present model prediction is in good agreement with the experimental results except for Mach numbers below this critical Mach number because the maximum of α_M is predicted in a region where the model is valid while the maximum of α_M in Fig. 4 was predicted at very low Mach numbers, where the model is not valid. In fact, the maximum of α_M will be observable theoretically for low values of b (or δ) (see Table 2).

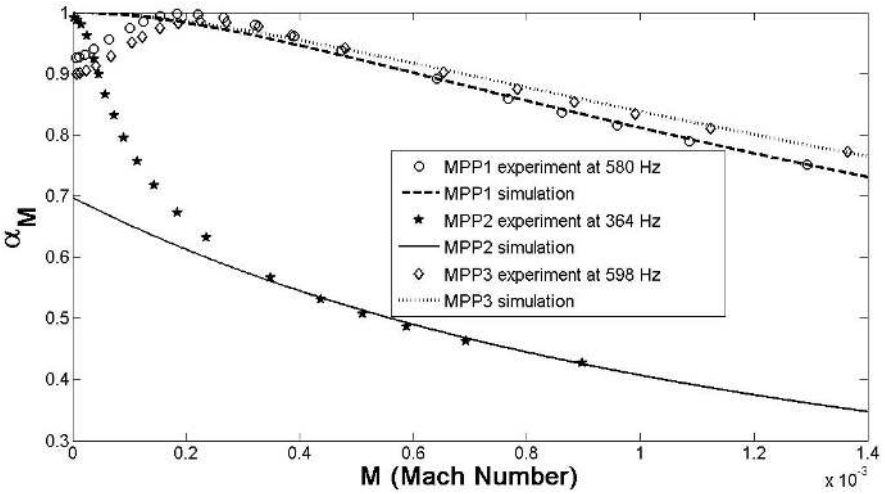

Figure 4: Absorption coefficient at resonance as a function of the Mach number in front of the MPP sample. Air cavity depth of 50 mm.

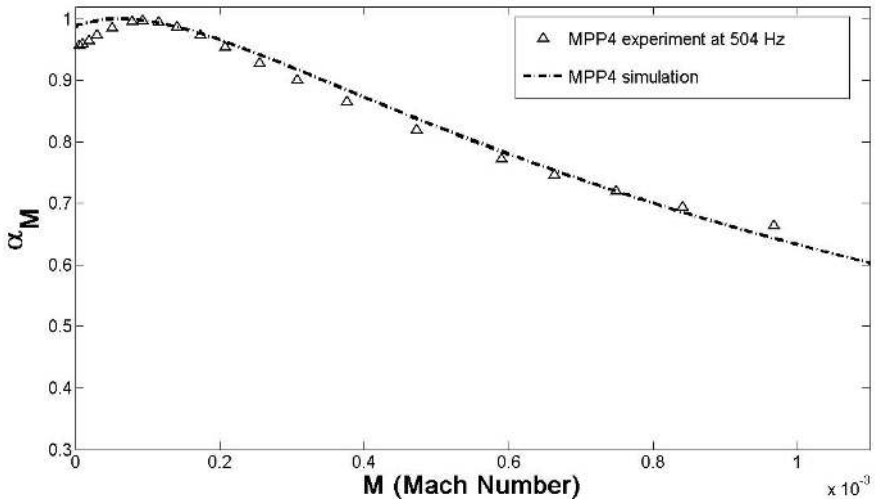

Figure 5: Experimental results of the maximum of absorption coefficient as a function of the Mach number in front of the panel. Air cavity depth of 50 mm.

4.2 Absorption coefficient as a function of frequency

Fig. 6 shows the comparison between experimental and simulations results (Maa[7], Hersh[5] and the present model) for the absorption coefficients of MPP1 at 145 dB in front of the panel (reference microphone) in the [200 - 1600 Hz] frequency range for an air cavity depth of 50 mm. The simulation of the present model and the measurement are in very good agreement. The first peak (around 564 Hz) is the perforation absorption peak and the second peak (around 900 Hz) is the result of the panel absorption peak resulting from the structural response of the panel coupled to an air cavity. The presented models and the measurements are in fairly good agreement except for the Hersh high sound model which does not fit well with the experiment results. Fig. 7a and Fig. 7b show the comparison between experimental and simulations results of

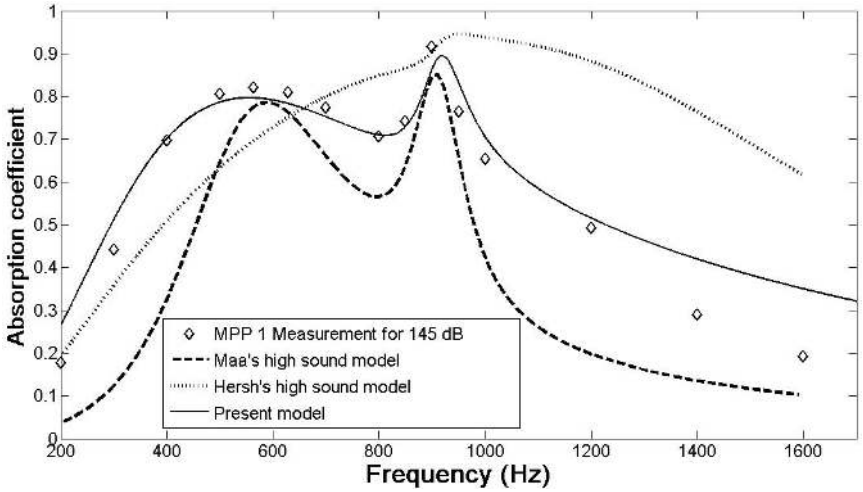

Figure 6: Comparison between the absorption coefficients of MPP1 at 145 dB (U=0.325m/s) on the reference microphone. Air cavity depth of 50 mm.

the surface impedance (resistance (a) and reactance (b)) of MPP1 at 145 dB in front of the panel (reference microphone) in the [200 - 1600 Hz] frequency range for an air cavity depth of 50 mm. The present model and the measurements are in very good agreement. On Fig. 7a, Maa's model underestimates the nonlinear resistance whereas Hersh's model agrees well with the experimental results except around the structural response frequency. On Fig. 7b, the models are in good agreement with the experimental results except for Hersh's model. Fig. 8 shows the comparison between experimental and simulation results (Maa[7], Hersh[5] and the present model) for the absorption coefficients of MPP3 at 145 dB in front of the panel (reference microphone) in the [200 - 1600 Hz] frequency range for an air cavity depth of 40 mm. The present model and the measurement results are in very good agreement. Fig. 9a and Fig. 9b show the comparison between experimental and simulations results for the surface impedance (resistance (a) and reactance (b)) of MPP3 at 145 dB in front of the panel (reference microphone) in the [200 - 1600 Hz] frequency range for an air cavity depth of 40 mm. On Fig. 9a, for the resistance part, below $800Hz$, the present model and the measurement results are in very good agreement. Yet beyond $800Hz$, the agreement is not good. This may imply considering a certain high-frequency-dependency of the nonlinear parameter for a more accurate prediction. However, as mentioned, for relatively high frequency, the absorption seems to be much more influenced by the imaginary part of the impedance. Maa's model underestimates the measurement results while Hersh's model tendency is good compared to the measurement results. On Fig. 9b, for the reactance part, the present model and Maa's model both agree accurately with the measurement results.

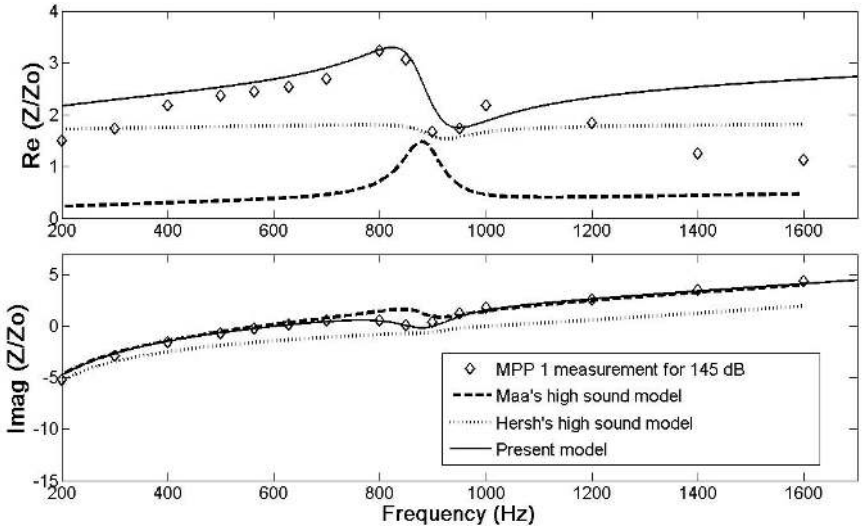

Figure 7: Comparison between the surface impedances (resistance (a) and reactance (b)) of MPP1 at 145 dB (U=0.325m/s) on the reference microphone. Air cavity depth of 50 mm.

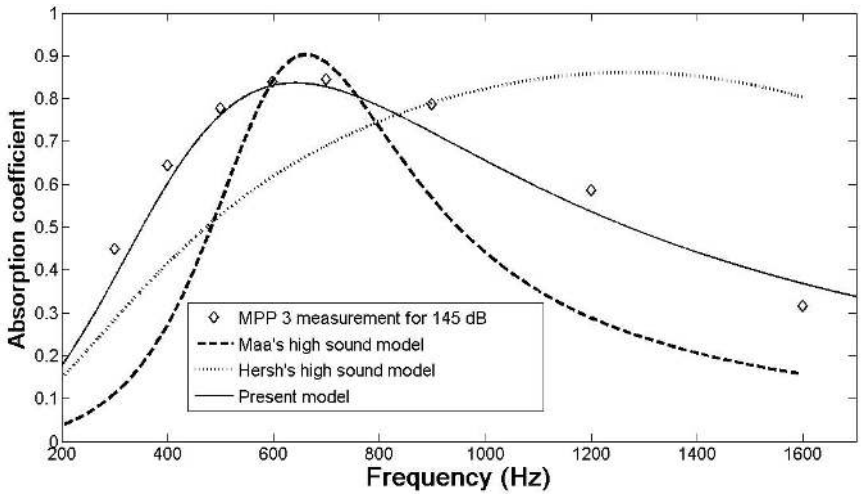

Figure 8: Comparison between the absorption coefficients of MPP3 at 145 dB (U=0.337m/s) on the reference microphone. Air cavity depth of 40 mm.

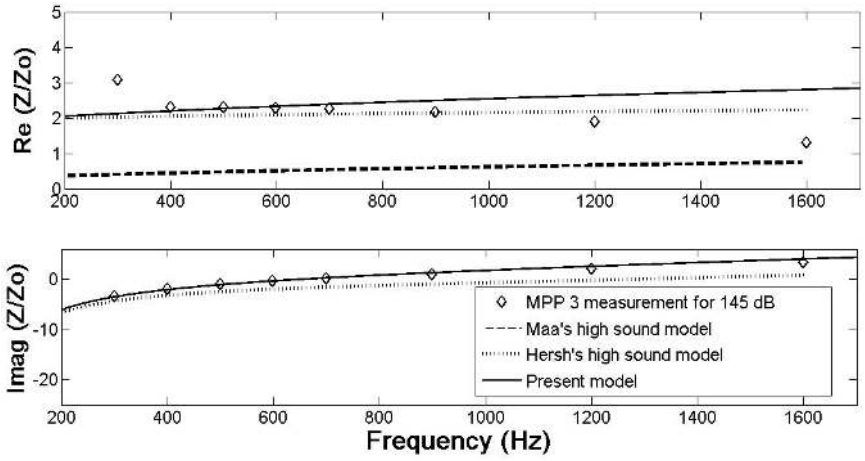

Figure 9: Comparison between the surface impedances (resistance (a) and reactance (b)) of MPP3 at 145 dB (U=0.337m/s) on the reference microphone. Air cavity depth of 40 mm.

Acknowledgements

The support grant for this work was provided by the Conseil Régional de Bourgogne. The authors would like to thank M. Bernard Adam and his team for their help in the experimental part of this work.

References

[1] D. Y. Maa, *Potential of Micro-perforated panel absorber*, Journal of Acoustical Society of America, Vol. 104, (1998), pp. 2861-2866.

[2] J.F. Allard, *Propagation of sound in porous media. Modelling sound absorbing materials*, Elsevier, New York, (1993), chap 10.

[3] U. Ingard, *On the Theory and Design of Acoustic Resonators*, Journal of Acoustical Society of America, Vol. 25, No. 6, (1953), pp. 1037-1061.

[4] U. Ingard, H. Ising, *Acoustic Nonlinearity of an Orifice*, Journal of Acoustical Society of America, Vol. 42, (1967), pp. 6-17.

[5] A. S. Hersh, B. E. Walker, J. W. Celano, *Helmholtz Resonator Impedance Model, Part I:Nonlinear Behavior*, American Institute of Aeronautics and Astronautics, Vol. 41, No. 5, (2003), pp. 795-808.

[6] T. H. Melling, *The acoustic Impedance of perforates at medium and high sound pressure levels*, Journal of Sound and Vibration, Vol. 29, No. 1, (1973), pp. 9-12.

[7] D. Y. Maa, *Micro-perforated panel at high sound intensity*, InterNoise, Yokohama Japan, (1994).

[8] P.M. Morse, *Vibration and Sound*, McGraw-Hill, New York, (1948).

[9] L. Rayleigh, *Theory of sound II*, MacMillan, New York, (1929).

[10] E. Buckingham, *On physically similar systems; Illustrations of the use of Dimensional Equations*, Physics Review Letters, Vol. 4, No. 4, (1914), pp. 345-376.

[11] Y. Auregan, M. Pachebat, *Measurement of the nonlinear behavior of acoustical rigid porous materials*, Physics of Fluids, Vol. 11, No. 6, (1999), pp. 1342-1345.

[12] J. D. McIntosh, R. F. Lambert, *Nonlinear wave propagation through rigid porous materials. I:Nonlinear parametrization and numerical solutions*, Journal of Acoustical Society of America, Vol. 88, No. 4, (1990), pp. 1939-1949.

[13] J. Y. Chung, D. A. Blaser, *Transfer function method of measuring in-duct acoustic properties. I Theory*, Journal of Acoustical Society of America, Vol. 68, No. 3, (1980), pp. 907-913.

[14] J-. P. Dalmont, *Acoustic impedance measurement. part I: a review*, Journal of Sound and Vibration, Vol. 243, No. 3, (2001), pp. 441-459.